Threshold-Based Pair Switching Scheme in SWIPT-Enabled Wireless Downlink System

Yuan Guo, Christodoulos Skouroumounis, and Ioannis Krikidis
IRIDA Research Centre for Communication Technologies
Department of Electrical and Computer Engineering, University of Cyprus
Email: {yguo0001, cskour03, krikidis}@ucy.ac.cy

***Abstract*—In this paper, we investigate a low complexity technique for simultaneous wireless information and power transfer (SWIPT) in the context of cellular networks, where the multiple-antenna user equipments (UEs) employ maximum ratio combining technique. In particular, our proposed technique allocates a subset of antennas for information decoding (ID), only when their post-combiner signal-to-interference ratio exceeds a certain threshold, while the remaining antennas are allocated for energy harvesting (EH). In contrast to conventional approaches, where an uncorrelated or a fully correlated interference is considered, we develop a realistic mathematical framework that accurately captures the interference correlation effects on the performance of the proposed technique. By using stochastic geometry tools, we derive analytical expressions for both the ID and EH success probability, as well as the joint ID and EH success probability. Our results demonstrate the impact of spatial interference correlation on both the ID and the EH success probability, and we establish the optimal threshold for the proposed antenna switching scheme, that maximizes the joint ID and EH success probability.**

***Index Terms*—SWIPT, interference correlation, stochastic geometry.**

I. Introduction

The concept of simultaneous wireless information and power transfer (SWIPT) is gradually becoming more and more compelling to efficiently exploit the received ambient radio-frequency (RF) signal, aiming to obtain both information and energy. Although information theoretic studies ideally assume that a receiver is able to decode information and harvest energy independently from the same signal, this approach has been previously regarded infeasible due to practical limitations [1]. Fortunately, the concept of SWIPT becomes feasible by splitting the received RF signal in two parts; one part is used for information transfer and another part is used for power transfer. The partitioning of the RF signal can be performed either in the time, the power, or the space domain [2].

The concept of SWIPT technology in the context of large-scale networks has been widely-investigated in the literature. In the context of cellular networks, the authors in [3] studied the performance limits of a three-nodes multiple-input-multiple-output (MIMO) broadcast system, with separate energy harvesting (EH) and information decoding (ID) receivers. A mathematical framework for stochastic geometry analysis of SWIPT-enabled MIMO systems was originally proposed in [4], and the trade-off between information rate and harvested power was demonstrated. In [5], the authors studied the joint analysis of harvested energy and downlink signal-to-interference-plus-noise ratio, while encompassing a realistic channel model that accounts for line-of-sight (LOS) and non-LOS links, different cell association criteria and directional beamforming. The concept of SWIPT in intelligent reflecting surface (IRS)-assisted cellular networks was investigated in [6], highlighting that the IRSs can facilitate in compensating the high RF signal attenuation over long distance and thereby establish effective energy harvesting/charging zones for hot-spot areas in their proximity. The majority of the above works focuses on SWIPT-enabled networks based on either power splitting (PS) or time switching (TS) protocols. Nevertheless, the strict synchronization requirement for the TS approach and the demand of an appropriate power-splitting circuit for the PS approach, escalate the hardware complexity and cost [7]. Antenna switching (AS), on the other hand, is a promising low-complexity alternative approach that has been overlooked.

The main performance-limiting factor in wireless systems is the existence of interference between the network's nodes. The interference is spatially correlated since it stems from a single set of transmitters, even in the presence of independent fading [8] [9]. While it has been long recognized that the correlated fading reduces the performance gain of multi-antenna communication systems, the concept of interference correlation has been overlooked until recently. Such spatial correlation of interference power affects the diversity gain of the system, especially in high path loss environment [8]. In [9], the authors also addressed interference correlation issues of the multiple-antenna users and characterized the performance of maximum ratio combining (MRC) in the presence of spatially-correlated interference across antennas. In [10], the authors characterized the spatio-temporal interference correlation as well as the joint coverage probability at two spatial locations in a cellular network and showed that the interference correlation and the joint coverage probability decrease with the increase of the mobile users' speed. Therefore, the analytical characterization of the diversity in wireless networks with interference, necessitates

This work has received funding from the European Research Council (ERC) under the European Union's Horizon 2020 research and innovation programme (Grant agreement No. 819819) and from the Marie Skłodowska-Curie project PAINLESS under the European Union's Horizon 2020 research and innovation programme (Grant agreement No. 812991). This work was also co-funded by the European Regional Development Fund and the Republic of Cyprus through the Research and Innovation Foundation, under the project INFRASTRUCTURES/1216/0017 (IRIDA).

the careful treatment of the interference correlation, otherwise the results may be misleading.

In this paper, we assess the effect of the SWIPT technique in the context of cellular networks, where the user equipments (UEs) are equipped with multiple antennas. The main contribution of this paper is the development of a novel threshold-based pair switching (TbPS) scheme to facilitate the UEs' allocation either for ID or for EH. In particular, based on the proposed scheme, each UE allocates a subset of its antenna elements for ID, only when the post-combiner signal-to-interference ratio (SIR) observed by this subset is beyond a certain threshold, while the remaining antenna elements are allocated for EH. In contrast to conventional approaches, where the interference power across the antennas elements is either assumed fully correlated or fully uncorrelated, we propose an analytical framework based on stochastic geometry that captures the impact of the spatially-correlated interference on the ID and EH performance of the considered system. In particular, the interference power received within each pair of antenna elements is assumed to be fully correlated, and the interference observed at the various pairs is considered to be independent. Based on the developed framework, we derive analytical expressions for the success probability of ID and EH, as well as for the joint success probability, i.e. ID and EH. Our results illustrate the effectiveness of our proposed low-complexity technique in satisfying the ID or/and EH constrains of a UE and demonstrate the impact of interference correlation on the achieved performance. Moreover, the optimal threshold that maximizes the joint ID and EH success probability is established.

Notation: $\mathbb{R}^d$ denotes the d dimensional Euclidean space; $\|x\|$ denotes the Euclidean norm of $x \in \mathbb{R}^d$; $\mathbb{P}[X]$ denotes the probability of the event X and $\mathbb{E}[X]$ represents the expected value of X; $\Gamma(\cdot)$, $\Gamma(\cdot,\cdot)$ and $\gamma(\cdot,\cdot)$ denote the complete, the upper incomplete and lower incomplete Gamma functions, respectively; ${}_2F_1(\cdot,\cdot;\cdot;\cdot)$ is the Gauss hypergeometric function; $\mathcal{H}(\cdot)$ is the Heaviside function and $\bar{\mathcal{H}}(x) = 1 - \mathcal{H}(x)$.

II. System Model

We consider a bi-dimensional wireless downlink cellular network. The locations of the base stations (BSs) are distributed based on a homogeneous Poisson Point Process (PPP) $\Phi = \{x_i \in \mathbb{R}^2\}$ with density of λ, where x_i denotes the spatial coordinates of the i-th node. Moreover, we consider the case where all BSs have single transmit antenna and all UEs are equipped with N receive antenna elements [8]. In addition, the locations of the UEs follow a uniform distribution of density $\lambda_U \gg \lambda$. Based on the Slivnyak's theorem and without loss of generality, we perform our analysis from the perspective of the typical UE, which is located at the origin [11]. Furthermore, we consider a distance-based association rule, where the typical UE is served by its closest BS at x_o, i.e. $\|x_o\| = \arg\min_{x_i \in \Phi} \|x_i\|$. Hence, the complementary cumulative distribution function (ccdf) of the distance R from a UE to its serving BS, is given by $\mathbb{P}[R \geq r] = \exp[-\pi\lambda r^2]$, and the probability density function (pdf) of the distance R, is given by [11] $f_r(r) = 2\pi\lambda r \exp(-\pi\lambda r^2)$, where follows from the fact that $f_r(r) = \frac{\mathrm{d}}{\mathrm{d}r}\left(1 - \mathbb{P}[R \geq r]\right)$.

All wireless signals are assumed to experience both large-scale path loss effects and small-scale fading; the network is considered to be interference-limited [8]. Regarding the small-scale fading, we assume Rayleigh fading with unit average power, where different links are assumed to be independent and identically distributed [5]. Therefore, the power gain of the channel between the k-th antenna element of a UE and a BS at $x_i \in \Phi$ is an exponential random variable with unit mean, i.e. $h_{k,i} \sim \exp(1)$. For the large-scale path loss between a receiver at X and a transmitter at Y, we assume an unbounded singular path loss model, i.e. $L(X,Y) = \|X - Y\|^\alpha$, where $\alpha > 2$ is the power path loss exponent. For simplicity, the path loss of the link between a BS at x_i and the typical UE is denoted as $L(x_i) = \|x_i\|^\alpha$.

Even though we assume that the channels between the BSs and each antenna element of a UE are independent with each other, the received interference across different antenna elements is correlated due to the common locations of the transmitter [8]. Motivated by the small distance between adjacent antenna elements of a UE, we divide the set of antenna elements into η pairs of two antenna elements, i.e. $\eta = N/2$. Such approach could capture the interference correlation between adjacent antenna elements and keep the tractability for the analytical framework. Specifically, we assume that the observed interference between each antenna element of a pair is fully-correlated, while the intended received signals and interference between pairs are considered uncorrelated. Then, based on the AS protocol [2], our proposed scheme assigns a subset of paired antenna elements, i.e. ν pairs, for ID purpose and the remaining $(\eta - \nu)$ pairs, for EH. Let S_k and $\mathcal{I}_k$ denote the power of the intended signal and observed interference at the k-th antenna element of a UE, respectively, where $k = \{1, \cdots, N\}$. Due to the full-correlation of the interference within each antenna pair, the interference across antennas in each pair is same, i.e. $\mathcal{I}_k = \mathcal{I}_{k+1} = \mathcal{I}_n$ where $k = 2n - 1$ and $n = \{1, \cdots, \eta\}$. Thus, based on the MRC technique, the SIR of the n-th antenna pair of the typical UE, is given by

$$\mathrm{SIR}_n = \frac{S_k + S_{k+1}}{\mathcal{I}_n} = \frac{\left(h_{k,o} + h_{k+1,o}\right) L^{-1}(x_o)}{\sum_{x_i \in \Phi \setminus o} h_{k,i} L^{-1}(x_i)}, \quad (1)$$

Regarding the selection of the number of antenna pairs, ν, we proposed a threshold-based approach based on the MRC [12]. Let Γ_ν denote the post-combiner SIR for the MRC at the receiver when ν pairs of antenna elements are selected, which is equal to $\Gamma_\nu = \sum_{j=1}^{\nu} \mathrm{SIR}_n$, where SIR_n is given by the expression (1). Based on the TbPS scheme, the number of antenna pairs, ν, is selected so that the post-combiner SIR at the receiver exceeds a certain predefined threshold γ_{th} (dB). Starting from the single-pair case, the TbPS scheme gradually raises the number of selected pairs aiming to satisfy the aforementioned condition. The previous actions are repeated until Γ_ν is greater than the threshold γ_{th}, while satisfying the constraint that at least one pair is allocated for EH.

$$\mathcal{L}_{\mathcal{I}_n}(s) = \exp\left(- \frac{2\pi\lambda s r_o^{2-\alpha}\ {}_2F_1\left(1, \frac{\alpha-2}{\alpha}; 2-\frac{2}{\alpha}; -s r_o^{-\alpha}\right)}{\alpha - 2}\right). \tag{2}$$

$$\frac{\partial \mathcal{L}_{\mathcal{I}_n}(s)}{\partial s} = \frac{2\mathcal{L}_{\mathcal{I}_n}(s)\pi r_o^2\lambda\left(2-\alpha-2(1+s r_o^{-\alpha})\ {}_2F_1\left(1, \frac{\alpha-2}{\alpha}; 2-\frac{2}{\alpha}; -s r_o^{-\alpha}\right)\right)}{(r_o^\alpha + s)(\alpha-2)\alpha} \tag{3}$$

III. SWIPT with Threshold-based Pair Switching technique

In this section, we analyse the performance of the proposed TbPS technique in the context of cellular networks, where the multi-antenna UEs employ the MRC technique in the presence of spatial interference correlation. Specifically, we characterize the ability of a UE to successfully decode the received signal and harvest sufficient energy. Based on the proposed low-complexity TbPS technique, analytical expressions for the ID, EH, and joint ID and EH success probability are derived by using tools from stochastic geometry.

A. Information Decoding Success Probability

Firstly, we evaluate the conditional cumulative distribution function (cdf) of SIR_n, i.e. $\mathbb{P}[\mathrm{SIR}_n < \Upsilon | x_o]$, where Υ is the decoding threshold and x_o is the location of the serving BS of the typical UE, which is useful for evaluating the ID, EH, and the joint ID and EH success probability. The following lemma evaluates the conditional cdf of the SIR at the n-th antenna pair of the typical UE.

Lemma 1. *The conditional cdf for the SIR of the n-th antenna pair, i.e. SIR_n, is given by*

$$F(\Upsilon|x_o) = 1 - \mathcal{L}_{\mathcal{I}_n}(s) + s\frac{\partial \mathcal{L}_{\mathcal{I}_n}(s)}{\partial s},$$

where $s = \Upsilon L(x_o)$, $\mathcal{L}_{\mathcal{I}_n}(s)$ and $\partial\mathcal{L}_{\mathcal{I}_n}(s)/\partial s$ are given in (2) *and* (3)*, respectively, and $r_o = \|x_o\|$.*

Proof. See Appendix A. □

The following Remark investigates a special case of Lemma 1, where $\alpha = 4$, which is a common practical value for path-loss exponent in outdoor urban environments.

Remark 1. *For the special case $\alpha = 4$, the Laplace transform and the derivative of the Laplace transform of the interference observed at the n-th antenna pair can be simplified as*

$$\mathcal{L}^*_{\mathcal{I}_n}(s) = \exp\left(-\pi\sqrt{s}\tan^{-1}\left(r_o^{-2}\sqrt{s}\right)\right),$$

and

$$\frac{\partial \mathcal{L}^*_{\mathcal{I}_n}(s)}{\partial s} = -\frac{\mathcal{L}^*_{\mathcal{I}_n}(s)\pi\lambda}{2}\left(\frac{r_o^2}{r_o^4+s} + \frac{\tan^{-1}\left(r_o^{-2}\sqrt{s}\right)}{\sqrt{s}}\right).$$

The ID success probability in the context of our proposed TbPS scheme can be formulated as

$$\begin{aligned}\mathcal{F}_{\mathrm{ID}}(\chi,\gamma_{th}) =& \mathbb{P}\left[\Gamma_1 \geq \chi\ \&\ \Gamma_1 \geq \gamma_{th}\right] \\ &+ \sum\nolimits_{v=2}^{\eta-2}\mathbb{P}\left[\Gamma_v \geq \chi\ \&\ \Gamma_{v-1} < \gamma_{th} < \Gamma_v\right] \\ &+ \mathbb{P}\left[\Gamma_{\eta-1} \geq \chi\ \&\ \Gamma_{\eta-2} < \gamma_{th}\right],\end{aligned}$$

where χ (dB) is the decoding threshold. Although the proposed scheme is suitable for any even number of antenna elements at the UEs, in this work we consider the scenario where $N = 6$ for tractability purposes. The aforementioned assumption holds for practical wireless devices that typically equipped with small number of antenna elements, due to space limitations and complexity constrains, e.g. smart phones, WiFi routers [9]. For this special case, the following proposition characterizes the resulting performance in terms of ID success probability.

Proposition 1. *For the special case where UEs are equipped with six antenna elements, i.e. $N = 6$, the ID success probability, $\mathcal{F}_{\mathrm{ID}}(\chi,\gamma_{th})$, is given by*

$$\mathcal{F}_{\mathrm{ID}}(\chi,\gamma_{th}) = \int_0^\infty \mathcal{T}_{\mathrm{ID}}(\chi,\gamma_{th},r) f_r(r)\mathrm{d}r, \tag{4}$$

where

$$\begin{aligned}\mathcal{T}_{\mathrm{ID}}(\chi,\gamma_{th},r) =& 1 - \bar{\mathcal{H}}(\chi-\gamma_{th})\int_0^\chi F(\chi-y|r)f(y|r)\mathrm{d}y \\ &- \mathcal{H}(\chi-\gamma_{th})\Big(F(\chi|r) - F(\gamma_{th}|r) \\ &+ F(\chi-\gamma_{th}|r)F(\gamma_{th}|r) \\ &+ \int_{\chi-\gamma_{th}}^\chi F(\chi-y|r)f(y|r)\mathrm{d}y\Big),\end{aligned}$$

$F(\Upsilon|x_o)$ is the conditional cdf of SIR_n, which is given in Lemma 1 , and $f(\Upsilon|x_o)$ is the conditional pdf of the SIR_n and can be calculated as $f(\Upsilon|x_o) = \partial F(\Upsilon|x_o)/\partial\Upsilon$.

Proof. See Appendix B. □

B. Energy Harvesting Success Probability

In this section, we investigate the EH success probability for our proposed TbPS scheme. Specifically, the EH success probability describes the ability of a UE to successfully harvest RF energy above a predefined reliability threshold Q (dBm) based on the practical application. Similar to [5], we consider a linear energy harvest (LEH) model[1], where the harvested energy is defined as the aggregate received signal power multiplied with the conversion efficiency ζ of the energy harvester. Moreover, in order to derive compact and insightful expressions for the EH success probability, the aggregate interference power harvested by the energy harvester is approximated by the mean interference power, denoted as $\bar{\mathcal{I}}$. The accuracy of the above-mentioned approximation is illustrated in the numerical results in Section V. Therefore, the mean interference power is given by [11]

$$\bar{\mathcal{I}} \triangleq \mathbb{E}_{h,\Phi}\left[\sum\nolimits_{x_i\in\Phi\setminus o} h_{k,i}L(x_i)^{-1}\right] = 2\pi\lambda\|x_o\|^{2-\alpha}(\alpha-2)^{-1}.$$

[1]Such LEH model is used for mathematical tractability and it is accurate for the intermediate input power of the energy harvester [13]. Moreover, the proposed mathematical framework serves as a useful guideline for more practical nonlinear EH models.

Then, based on the number of selected pairs, ν, the EH success probability achieved by the TbPS scheme, can be formulated as,

$$\mathcal{F}_{\mathrm{EH}}(Q,\gamma_{th}) = \mathbb{P}[\Gamma_1 \geq \gamma_{th}]\mathbb{P}\left[\zeta\left(\sum_{j=1}^{\eta} S_{2j-1}+S_{2j}+2\bar{\mathcal{I}}\right)\geq Q\right] + \sum_{v=2}^{\eta-2}\mathbb{P}[\Gamma_{v-1}<\gamma_{th}<\Gamma_v]\mathbb{P}\left[\zeta\left(\sum_{j=v+1}^{\eta} S_{2j-1}+S_{2j}+2\bar{\mathcal{I}}\right)\geq Q\right] + \mathbb{P}\left[\Gamma_{\eta-2}<\gamma_{th}\right]\mathbb{P}\left[\zeta\left(S_{2\eta-1}+S_{2\eta}+2\bar{\mathcal{I}}\right)\geq Q\right],$$

where Q is the reliability threshold. For the special case where $N = 6$, the following proposition characterizes the resulting performance in terms of EH success probability.

Proposition 2. *For the special case where UEs are equipped with six antenna elements, i.e. $N = 6$, the EH success probability, $\mathcal{F}_{\mathrm{EH}}(Q,\gamma_{th})$, is given by*

$$\mathcal{F}_{\mathrm{EH}}(Q,\gamma_{th}) = \int_0^{\infty} \mathcal{T}_{\mathrm{EH}}(Q,\gamma_{th},r) f_r(r)\mathrm{d}r, \tag{5}$$

where

$$\mathcal{T}_{\mathrm{EH}}(Q,\gamma_{th},r_o) = \bar{F}(\gamma_{th}|r_o)H_2(Q|r_o) + F(\gamma_{th}|r_o)H_1(Q|r_o),$$
$$H_1(Q|r_o) = \Gamma\left(2,\ell(r_o,2)\right)\mathcal{H}\big(r_o-\gamma(1)\big)+\bar{\mathcal{H}}\big(r_o-\gamma(1)\big),$$
$$H_2(Q|r_o) = \frac{\Gamma\left(4,\ell(r_o,4)\right)}{\Gamma(4)}\mathcal{H}\big(r_o-\gamma(2)\big)+\bar{\mathcal{H}}\big(r_o-\gamma(2)\big),$$

$\bar{F}(\cdot) = 1-F(\cdot)$, $\ell(x,y) = L(x)(\bar{Q}-y\bar{\mathcal{I}})$, $\bar{Q} = Q/\zeta$, $\gamma(y) = \left(\frac{4y\pi\lambda}{\bar{Q}(\alpha-2)}\right)^{\frac{1}{\alpha-2}}$.

Proof. See Appendix C. □

C. Joint ID and EH Success Probability

In this section, we discuss the trade-off between the ID and the EH in the context of the TbPS scheme, by studying the joint ID and EH success probability [5]. Specifically, the joint ID and EH success probability, $\mathcal{F}_{\mathrm{ID\&EH}}(\chi,Q,\gamma_{th})$, refers to the ability of a UE to simultaneously satisfy both the ID and EH threshold. Hence, $\mathcal{F}_{\mathrm{ID\&EH}}(\chi,Q,\gamma_{th})$ can be evaluated as

$$\mathcal{F}_{\mathrm{ID\&EH}}(\chi,Q,\gamma_{th}) = \mathbb{P}[\Gamma_1 \geq \chi \& \Gamma_1 \geq \gamma_{th}]\mathbb{P}\left[\sum\nolimits_{j=1}^{\eta} S_{2j-1}+S_{2j}+2\bar{\mathcal{I}}\geq\bar{Q}\right] + \sum_{v=2}^{\eta-2}\mathbb{P}[\Gamma_\nu \geq \chi\,\&\,\Gamma_{v-1}<\gamma_{th}<\Gamma_v]\mathbb{P}\left[\sum_{j=v+1}^{\eta} S_{2j-1}+S_{2j}+2\bar{\mathcal{I}}\geq\bar{Q}\right] + \mathbb{P}\left[\Gamma_{\eta-1}\geq\chi\&\Gamma_{\eta-2}<\gamma_{th}\right]\mathbb{P}\left[S_{2\eta-1}+S_{2\eta}+2\bar{\mathcal{I}}\geq\bar{Q}\right].$$

In the following proposition, we evaluate the joint ID and EH success probability for the special case with $N = 6$ antennas.

Proposition 3. *For the special case where UEs are equipped with six antenna elements, i.e. $N = 6$, the joint ID and EH success probability is given by*

$$\mathcal{F}_{\mathrm{ID\&EH}}(\chi,Q,\gamma_{th}) = \int_0^{\infty} \mathcal{T}_{\mathrm{ID\&EH}}(\chi,Q,\gamma_{th},r) f_r(r)\mathrm{d}r,$$

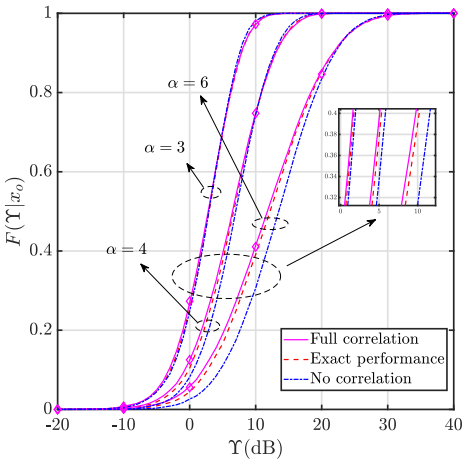

Fig. 1. The conditional cdf of SIR_n for different $\alpha \in \{3,4,6\}$; $r_o = 30$ m.

where

$$\mathcal{T}_{\mathrm{ID\&EH}}(\chi,Q,\gamma_{th},r) = \mathcal{H}(\chi-\gamma_{th})\Big(H_2(Q|r)\bar{F}(\chi|r) + H_1(Q|r)F(\gamma_{th}|r)\int_0^{\gamma_{th}} F(\chi-y|r)f(y|r)\mathrm{d}y\Big) + \bar{\mathcal{H}}(\chi-\gamma_{th})\Big(H_2(Q|r)\bar{F}(\gamma_{th}|r) + H_1(Q|r) \times F(\gamma_{th}|r)\left(1-H_1(Q|r)\right)\int_0^{\chi} F(\chi-y|r)f(y|r)\mathrm{d}y\Big),$$

Proof. The proof follows the similar methodology with the Proposition 1 and Proposition 2, and hence is omitted. □

IV. Numerical and Simulation Results

In this section, we provide analytical and simulated results to validate the accuracy of our model and illustrate the performance of the TbPS scheme. Unless otherwise stated, in our results we consider the following parameters: the density λ of the BSs is $\lambda = 1/(R_{cell}^2\pi)$, where $R_{cell} = 40$ m, $\alpha = 3$ and $\zeta = 0.7$ [5].

Fig. 1 demonstrates the conditional cdf of SIR_n for different path loss exponents. Initially, the agreement between the theoretical curves (solid and dashed lines) and the simulation results (markers) validates our mathematical analysis. In order to demonstrate the impact of the interference correlation on the performance achieved by the TbPS scheme and validate the accuracy of the adopted assumptions, we numerically evaluate the scenario, where the interference power observed within each antenna pair is correlated but not equal (denoted as "Exact performance"), i.e. $\mathcal{I}_k \neq \mathcal{I}_{k+1}$. Moreover, we evaluate the performance achieved under uncorrelated interference, where interference received at different antenna elements is independent with each other (denoted as "No correlation"), which is used as benchmark for comparing with our proposed mathematical framework. We can easily observe that the performance achieved by using the adopted assumptions provides a tight upper bound for the exact performance, with lower

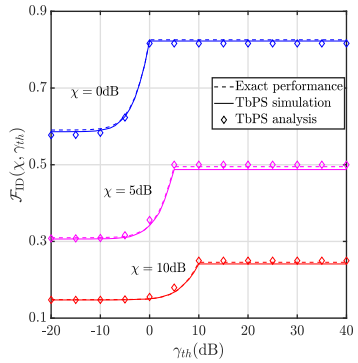

Fig. 2. ID success probability versus the threshold γ_{th} for different $\chi \in \{0, 5, 10\}$ dB.

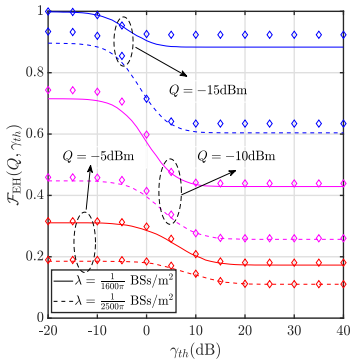

Fig. 3. EH success probability versus the threshold γ_{th} for different $Q \in \{-15, -10, -5\}$ dBm.

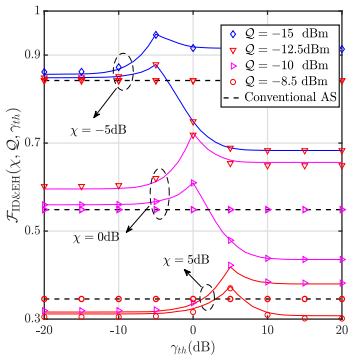

Fig. 4. Joint ID and EH success probability versus the threshold γ_{th} for different $\chi \in \{-5, 0, 5\}$ dB and $Q \in \{-15, -12.5, -10, -8.5\}$ dBm.

computational complexity. On the other hand, by ignoring the existence of spatial correlation between interference, it leads to a large deviation from the exact performance, especially, for higher path loss exponents. This was expected since, in dense urban areas, i.e. high path loss exponents, the aggregate interference is mainly composed by the interference caused by the closest interfering BS. Hence, if an antenna fails to decode the received signal, then the rest antenna will fail to decode the received signal with high probability, due to the existence of interference correlation.

Fig. 2 illustrates the effect of the threshold γ_{th} on the ability of a UE to successfully decode the received signal power. In particular, Fig. 2 plots the ID success probability with respect to the threshold γ_{th} for different decoding thresholds $\chi \in \{0, 5, 10\}$ dB. It can be observed that there exist minimum gaps between our analytical results and the exact performance. Moreover, we can easily observe that the ability of a UE to successfully decode the received signal power increases with the increase of the predefined threshold γ_{th}. This was expected since, the increase of γ_{th} results in an increased number of antenna elements that perform ID, and consequently, the ability to successfully decode the received signal power is enhanced. However, beyond a critical value of γ_{th}, which is equal to $\gamma_{th} = \chi$, the ID success probability remains constant. This can be explained by the fact that, for large values of γ_{th}, a UE is unable to assign an additional pair of antennas for the ID due to the constrain of the existence of at least one pair of antennas for EH, i.e. the performance could be further boosted for the receiver with more pairs of antenna elements. Moreover, by increasing the decoding threshold χ, the ID performance drops, which is from fact that greater decoding threshold requires higher post-combiner SIR to achieve the same success probability.

Similarly, Fig. 3 illustrates the effect of γ_{th} on the EH success probability for different reliability thresholds $Q \in \{-15, -10, -5\}$ dBm and different density of BSs $\lambda \in \{1/(1600\pi), 1/(2500\pi)\}$. First it can be observed that denser BS deployments can boost the EH success probability based on the proposed TbPS technique. This is based on the fact that the increasing number of active BSs in the network results in a higher aggregated received signal power at the UEs, which can be harvested. Moreover, as expected, the harvested energy of UE decreases as the predefined threshold γ_{th} increases, since the number of antenna elements allocated for energy harvesting reduces, and hence the EH success probability drops. Moreover, Fig. 3 also demonstrates the impact of the considered approximation regarding the observed interference on the EH success probability. The small deviation from the simulation results shows that the overall network interference can be effectively approximated by the mean interference power, without being significantly deficient in accuracy.

Fig. 4 shows the impact of the threshold γ_{th} on the ability of a UE to simultaneously satisfy the requirements for both ID and EH procedures. It is interesting to note that, by increasing the threshold γ_{th}, the ability of a user to simultaneously satisfy the ID and EH constrains increases. This is because, as the value of the threshold γ_{th} increases, the proposed TbPS scheme allocates a higher number of antenna elements for the ID part. Hence, the ability of a UE to successfully decode the received signal is significantly improved, while its ability to harvest energy is slightly reduced. However, beyond the critical point $\gamma_{th} = \chi$, the ability of a user to simultaneously satisfy the ID and EH constrains decreases. As indicated in Fig. 2 and Fig. 3, the ability of a user to successfully decode the received signal beyond a threshold equal to $\gamma_{th} = \chi$, remains constant, while the ability to harvest energy is reducing, and hence the joint ID and EH success probability is decreasing. Finally, we numerically investigate the conventional AS scheme, where half number of antennas are used for ID and half for EH [2]. It can be observed that, the performance achieved with our proposed technique outperforms that of the conventional scheme in terms of the optimal joint ID and EH success probability. Moreover, the proposed TbPS scheme is able to satisfy various ID and EH requirements of practical applications, by adjusting the predefined threshold.

V. Conclusion

In this paper, we investigated a low-complexity antenna pair-switching technique between decoding/harvesting for

SWIPT in wireless downlink communications system with spatially correlated interference between nearby antenna elements. In particular, the proposed scheme allocates a subset of antenna pairs for ID and the remaining antenna pairs for EH, based on a predefined threshold. By leveraging stochastic geometry tools, we investigated the ID and EH performance of SWIPT-enabled UEs from a macroscopic point-of-view. More specifically, we first evaluated the expression of the conditional cdf of SIR observed by each antenna elements pair of UEs. Then, analytical expressions for the achieved ID success probability as well as the EH success probability were investigated, and analytical expressions for the joint ID and EH success probability have also been derived. Our results show that based on proposed TbPS technique, the denser BS deployments can boost the EH. Moreover, our results have shown the data-energy trade-off in the TbPS scheme, highlighting the existence of an optimum threshold that maximizes the joint ID and EH success probability. Aiming to further enhance the achieved performance of SWIPT-enabled cellular networks, a future extension of this work is to investigate other antenna switching policies.

Appendix A
Proof of Lemma 1

Based on the expression (1), the conditional cdf of SIR_n, can be expressed as

$F(\Upsilon|x_o) = \mathbb{P}\left[h_{k,o} + h_{k+1,o} \leq L(x_o)\mathcal{I}_n\Upsilon\right] = \mathbb{E}\big[\gamma\left(2, s\mathcal{I}_n\right)\big]$,

where $s = \Upsilon L(x_o)$, and (6) follows from the fact that the sum of two exponential random variables follows the Gamma distribution [9]. Then, based on the moment generating function and $\gamma(x,y) = \Gamma(x) - (x-1)!e^{-y}\sum_{k=0}^{y-1}\frac{y^k}{k!}$, the final expression can be derived, where

$$\begin{aligned}\mathcal{L}_{\mathcal{I}_n}(s) &= \mathbb{E}\left[\exp\left(-\sum\nolimits_{x_i\in\Phi^{\setminus 0}}\frac{h_{k,i}s}{L(x_i)}\right)\right]\\ &= \exp\left(2\pi\lambda\int_{\|x_o\|}^{\infty}\left(\phi(x,s)-1\right)x\mathrm{d}x\right),\end{aligned} \tag{6}$$

where (6) is obtained from the Probability Generating Function (PGFL) of PPPs [11] and $\phi(x,s)$ is

$\phi(x,s) = \mathbb{E}_h\big[\exp\left(-h_{k,i}sL^{-1}(x)\right)\big] = \left(1+sL^{-1}(x)\right)^{-1}$.

Therefore, by evaluating the integral and derivative, the expressions in Lemma 1 can be derived.

Appendix B
Proof of Proposition 1

For the special case where $N=6$, the ID success probability, can be formulated as

$$\begin{aligned}\mathcal{F}_{\mathrm{ID}}(\chi,\gamma_{th}) = 1 &- \mathbb{P}[\mathrm{SIR}_1 < \chi,\ \mathrm{SIR}_1 \geq \gamma_{\mathrm{th}}]\\ &- \mathbb{P}[\mathrm{SIR}_1 + \mathrm{SIR}_2 < \chi,\ \mathrm{SIR}_1 < \gamma_{\mathrm{th}}].\end{aligned}$$

For the scenario where $\gamma_{th} < \chi$, the above expression can be re-written as

$$\begin{aligned}\mathcal{F}_{\mathrm{ID}}(\chi,\gamma_{th}) =& 1 - \mathbb{P}\left[\gamma_{th} \leq \mathrm{SIR}_1 < \chi\right]\\ &- \mathbb{P}\left[\mathrm{SIR}_1 < \chi\ - \mathrm{SIR}_2 | \chi\ - \mathrm{SIR}_2 \leq \gamma_{\mathrm{th}}\right]\\ &- \mathbb{P}\left[\mathrm{SIR}_1 < \gamma_{\mathrm{th}} | \gamma_{\mathrm{th}} \leq \chi\ - \mathrm{SIR}_2\right],\end{aligned}$$

while for $\gamma_{th} \geq \chi$, is given by

$$\begin{aligned}\mathcal{F}_{\mathrm{ID}}(\chi,\gamma_{th}) =& 1 - \mathbb{P}\left[\mathrm{SIR}_1 < \chi\ - \mathrm{SIR}_2\ \&\ \mathrm{SIR}_1 \leq \gamma_{\mathrm{th}}\right]\\ =& 1 - \mathbb{P}\left[\mathrm{SIR}_1 < \chi\ - \mathrm{SIR}_2\right].\end{aligned}$$

Then, by using the cdf of SIR_n, which is derived in Lemma 1, the final expression for $\mathcal{F}_{\mathrm{ID}}(\chi,\gamma_{th})$ can be derived.

Appendix C
Proof of Proposition 2

For the considered scenario, i.e. $N=6$, the TbPS scheme either assigns a single or two pairs of antenna elements for energy harvesting, based on the number of antenna elements that is selected for the ID part of the system. For the case where the TbPS scheme assigns two antenna pairs for ID, i.e. $\nu = 2$, then a single pair is allocated for EH. In this case, the EH success probability can be calculated as

$$H_1(Q|x_o) = \mathbb{P}[S_k + S_{k+1} + 2\bar{\mathcal{I}} \geq \bar{Q}|x_o],$$

where $\bar{Q} = Q/\zeta$. Similar with the proof of Lemma 1, for the case where $\bar{\mathcal{I}} < \bar{Q}/2$, we have the condition that $\|x_o\| \geq \left(4\pi\lambda(\alpha-2)^{-1}/\bar{Q}\right)^{1/(\alpha-2)}$ and hence,

$$\begin{aligned}H_1(Q|x_o) &= \mathbb{P}\left[S_k + S_{k+1} \geq \bar{Q} - 2\bar{\mathcal{I}}|x_o\right]\\ &= \Gamma\left(2, L(x_o)(\bar{Q} - 2\bar{\mathcal{I}})\right),\end{aligned} \tag{7}$$

where (7) is from the same methodology of (a) in Lemma 1. Furthermore, for the case, where $2\bar{\mathcal{I}} \geq \bar{Q}$, we have $\|x_o\| \leq \left(4\pi\lambda(\alpha-2)^{-1}/\bar{Q}\right)^{1/(\alpha-2)}$ and $H_1(Q|x_o) = 1$. Hence, the final expression of $H_1(Q|x_o)$ is derived. For the case where two pairs of antenna elements are used for EH, the EH success probability can be calculated as

$$H_2(Q|x_o) = \mathbb{P}[\sum\nolimits_{j=0}^{3} S_{k+j} + 4\bar{\mathcal{I}} \geq \bar{Q}|x_o].$$

The proof of $H_2(Q|x_o)$ follows similar methodology. Finally, by multiplying the probability of ν and following the similar methodology used in proof of Proposition 1, the Proposition 2 is proven.

References

[1] P. Grover and A. Sahai, "Shannon meets Tesla: Wireless information and power transfer," in *IEEE Int. Symp. on Inf. Theory*, Jun. 2010, pp. 2363–2367.

[2] I. Krikidis, S. Timotheou, S. Nikolaou, G. Zheng, D. W. K. Ng, and R. Schober, "Simultaneous wireless information and power transfer in modern communication systems," *IEEE Commun. Mag.*, vol. 52, no. 11, pp. 104–110, Nov. 2014.

[3] R. Zhang and C. K. Ho, "MIMO broadcasting for simultaneous wireless information and power transfer," *IEEE Trans. Wireless Commun.*, vol. 12, no. 5, pp. 1989–2001, May 2013.

[4] T. Tu Lam, M. Di Renzo, and J. P. Coon, "System-level analysis of SWIPT MIMO cellular networks," *IEEE Commun. Lett.*, vol. 20, no. 10, pp. 2011–2014, Oct. 2016.

[5] M. Di Renzo and W. Lu, "System-level analysis and optimization of cellular networks with simultaneous wireless information and power transfer: Stochastic geometry modeling," *IEEE Trans. Veh. Technol.*, vol. 66, no. 3, pp. 2251–2275, Mar. 2017.

[6] Q. Wu and R. Zhang, "Weighted sum power maximization for intelligent reflecting surface aided SWIPT," *IEEE Wireless Commun. Lett.*, vol. 9, no. 5, pp. 586–590, May 2020.

[7] I. Krikidis, S. Sasaki, S. Timotheou, and Z. Ding, "A low complexity antenna switching for joint wireless information and energy transfer in MIMO relay channels," *IEEE Trans. Commun.*, vol. 62, no. 5, pp. 1577–1587, May 2014.

[8] M. Haenggi, "Diversity loss due to interference correlation," *IEEE Commun. Lett.*, vol. 16, no. 10, pp. 1600–1603, Oct. 2012.

[9] R. Tanbourgi, H. S. Dhillon, J. G. Andrews, and F. K. Jondral, "Effect of spatial interference correlation on the performance of maximum ratio combining," *IEEE Trans. Commun.*, vol. 13, no. 6, pp. 3307–3316, Jun. 2014.

[10] S. Krishnan and H. S. Dhillon, "Spatio-temporal interference correlation and joint coverage in cellular networks," *IEEE Trans. Wireless Commun.*, vol. 16, no. 9, pp. 5659–5672, Sep. 2017.

[11] M. Haenggi, *Stochastic Geometry for Wireless Networks.* Cambridge University Press, 2012.

[12] F. Benkhelifa and M. Alouini, "Prioritizing data/energy thresholding-based antenna switching for SWIPT-enabled secondary receiver in cognitive radio networks," *IEEE Trans. Commun.*, vol. 3, no. 4, pp. 782–800, Dec. 2017.

[13] O. L. A. López, H. Alves, R. D. Souza, and S. Montejo-Sánchez, "Statistical analysis of multiple antenna strategies for wireless energy transfer," *IEEE Trans. Commun.*, vol. 67, no. 10, pp. 7245–7262, Oct. 2019.